Plasma diagnostics at electron cyclotron resonance ion sources by injection of laser ablated fluxes of metal atoms

V. Mironov
Joint Institute for Nuclear Research, PPL JINR, Dubna, Moscow Region, 141980, Russia

S. Runkel
Institut für Angewandte Physik der Johann Wolfgang Goethe-Universität, Robert-Mayer-Strasse 2-4, D-60054 Frankfurt am Main, Germany

K. E. Stiebing[a)]
Institut für Kernphysik der Johann Wolfgang Goethe-Universität, August Euler Straße 6, D60486, Frankfurt am Main, Germany

O. Hohn
Institut für Angewandte Physik der Johann Wolfgang Goethe-Universität, Robert-Mayer-Strasse 2-4, D-60054 Frankfurt am Main, Germany

G. Shirkov
Joint Institute for Nuclear Research, PPL JINR, Dubna, Moscow Region, 141980, Russia

H. Schmidt-Böcking
Institut für Kernphysik der Johann Wolfgang Goethe-Universität, August Euler Straße 6, D60486, Frankfurt am Main, Germany

A. Schempp
Institut für Angewandte Physik der Johann Wolfgang Goethe-Universität, Robert-Mayer-Strasse 2-4, D-60054 Frankfurt am Main, Germany

(Received 1 December 2000; accepted for publication 9 February 2001)

Short pulses of neutral particles generated by laser ablation of metal targets have been injected into the Frankfurt 14 GHz electron cyclotron resonance (ECR) ion source. Rise/fall times of pulses of highly charged ions of Cd and Mg were registered as a function of microwave power and gas pressure. From a comparison of the measured data to numerical simulations, values of the electron density and the temperature in the ECR plasma were estimated to be about $0.75\times10^{12}\,\mathrm{cm}^{-3}$ and a few keV. The effective electron temperature increases with increasing microwave power and decreases with increasing gas pressure. The electron density is only a weak function of the microwave power, but increases significantly with the gas pressure. In the Ar/O_2 gas-mixing mode of operation, an improved confinement of lowly charged ions was observed. [DOI: 10.1063/1.1361087]

I. INTRODUCTION

Electron cyclotron resonance ion sources (ECRIS) are successfully used as injectors of highly charged ions in a variety of accelerator facilities.[1] The underlying physical processes are quite complicated, and continuous efforts are undertaken by the ECRIS community to gather more information about the processes in the source plasma. A few years ago, a promising tool for the diagnostics of ECR discharges had been suggested.[2] This is the injection of short pulses of neutral particles, created by laser ablation of metal targets, into the source plasma. By observing the dynamics of the extracted pulses of ions in defined charge states, one is able to estimate various parameters of the plasma, such as, e.g., the effective temperature and density of its electron component. In this way, the reaction of the ECR plasma to changes of internal parameters, as well as the influence of special tools, such as gas mixing, biased electrode, etc. can be investigated. Besides this, the injection of laser-ablated fluxes into ECR plasmas is a promising way to produce beams of highly charged metal ions.

Laser ablation is an explosive type of evaporation of target material by short powerful laser pulses, followed by the creation of a dense hot plasma near the target surface. After being created and heated the plasma expands into the vacuum where the recombination of ions takes place. In this way intense short fluxes of particles of virtually any solid material can be formed. Ablation occurs if the power density of the focused laser beam exceeds a defined threshold value. These thresholds are different for different target materials and vary in the range of 10^7–10^9 W/cm^2. For YAG:Nd^{3+} laser systems with up to 100 mJ energy in *Q*-switched pulses, this implies that the size of the laser beam on the target surface should be of the order of 1 mm^2. Then, particle fluxes with total contents of about 10^{14}–10^{15} particles per pulse[3] are ejected from the target. The maximum of the velocity distribution of the particles lies at around 10^6 cm/s, their time spreads are in the order of $\cong 10\ \mu$s at a distance of

[a)]Electronic mail: stiebing@alpha.ikf.physik.uni-frankfurt.de

5 cm from the target. If one uses the laser beam intensity close to the threshold for ablation, these pulses consist to 90% of neutral particles. The total number of emitted particles increases with increasing laser-beam energy.

The time spread of these primary particle pulses is determined by the variation of the velocities of the ejected particles. It is directly proportional to the distance from the target. When the particles hit the surface of the vacuum chamber, they stick to the wall with a probability that depends on the type of particle, the angle of incidence, the particle energy, and the properties of the surface. Some of the particles will be reflected from the surface[4] with reflection coefficients in the order of 10%–30% for laser-ablation systems similar to the one used in the present experiments.[5] The pulse width of the particle flux into the plasma is mainly determined by these sticking rates of metallic atoms and ions to the walls. It is short enough (about 100 μs) compared to typical ionization/confinement times for highly charged ions in ECR plasmas, which are in the range of a few milliseconds.[1]

Crossing the plasma of the ECR discharge, those neutral particles, which are ionized, are then trapped inside the plasma and increase their charge step by step in ion-electron collisions. After their extraction and charge separation, the time structure of the pulsed currents of highly charged ions (HCI) provides information on these processes in the plasma. In particular, the rise times, as well as the amplitudes of the extracted current for the individual ion charge states are of interest.

The laser-ablation experiments reported here have been carried out at the Frankfurt 14 GHz ECRIS. Cadmium and magnesium targets were used, and the time dependence of the pulsed currents has been detected for nonoverlapping charge states of these metal ions as a function of the microwave power and the gas pressure. The influence of the biased electrode and of gas mixing has also been examined. The ion currents of the support-gas elements were registered to investigate their response to the injection. This work is a continuation of our previous study,[6] where Cd and Zn atoms were injected into the Frankfurt ECRIS.

II. EXPERIMENTAL SETUP

The Frankfurt 14 GHz ECRIS is described in detail elsewhere.[7] In its present configuration, a metal-dielectric structure (Al_2O_3/Al) is inserted into the plasma chamber,[8] which assists us in increasing the output of the highest charge states, at the same time decreasing the output of ions with lower charge states ($Z \leq 8$ for argon). The biased disk has been replaced by a ∅3 mm stainless steel rod inserted axially into the plasma chamber from the microwave injection side of the source. It was found that such a biased electrode works as good as the ∅28 mm biased disk used before[9] (see also Ref. 10).

To inject neutral particles into the ECR plasma, a metal (cadmium or magnesium) target was located inside the source chamber at the microwave injection side near the chamber wall (Fig. 1). The target surface was directed such that the angle between the source axis and the normal to the target surface was 150°. The laser beam entered the chamber through a vacuum window. It was focused onto the target by a lens with a focal length of 110 mm. The target-lens system was located inside one of the two 17° vacuum ports of the source.[11] In this configuration, the ablated fluxes of neutral particles had to be reflected by the plasma chamber walls before they could enter the ECR plasma. This avoids disturbances of the plasma by the direct fluxes of the ablated particles.

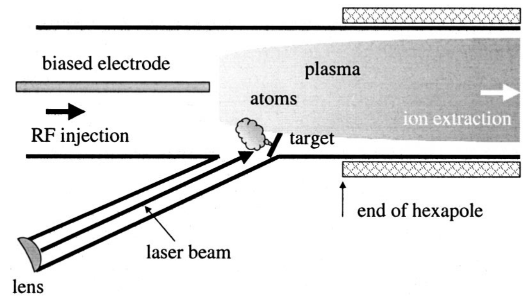

FIG. 1. Experimental setup.

An YAG:Nd^{3+} laser system was used with a wavelength of 1.06 μm, a pulse width of 15 ns (Q-switched mode of operation) and with up to 30 mJ energy per pulse. In the experiments described here, we used only single shots of the laser system. The laser beam energy was controlled by the voltage of the flash-lamp discharge battery.

The pulsed ion currents were detected after the 90° analyzing magnet in a Faraday cup of impedance of 50 Ω. The time dependence of the pulsed currents was registered by an oscilloscope, which was synchronized by the trigger signal of the laser Q-switch unit. The oscillograms were recorded by means of a digital camera.

The extraction voltage of the source was 25 kV throughout all experiments. The beam transport optics was optimized for each individual ion charge state under investigation. Only when measuring charge state distributions (CSD), the optical conditions remained fixed. In the given configuration, the source output was very sensitive to the beam transport tuning. In the extracted dc currents, Cd^{Z+} ions were observed even without laser ablation. This was due to the continuous sputtering of the target by the ECR plasma. After a few days of operation with a Cd target mounted in the source, a certain level of contamination of the chamber with Cd metal layers was observed, which remained even after removing the target out of the source. These dc currents never exceeded the level of 100 nA. They have to be compared to currents of (15–40) μA of Ar^{8+} ions and 1–2 μA of Cd^{18+} pulse amplitudes. However, the dc currents were useful to optimize the beam optics for the detection of pulsed currents of Cd^{Z+} ions. The CSD for dc currents of Cd ions peaked around (21+). dc currents of magnesium ions were beyond the limits of detection. For the measurement of pulsed currents of Mg^{Z+} ions, the optics was optimized to transport Ar ions with approximately the same M/Q ratio.

The experiments have been performed with pure argon as a working gas used to sustain the ECR discharge. Pure O_2 and Ar–O_2 gas mixing have also been examined; however, no satisfactory stability in the extracted currents could be

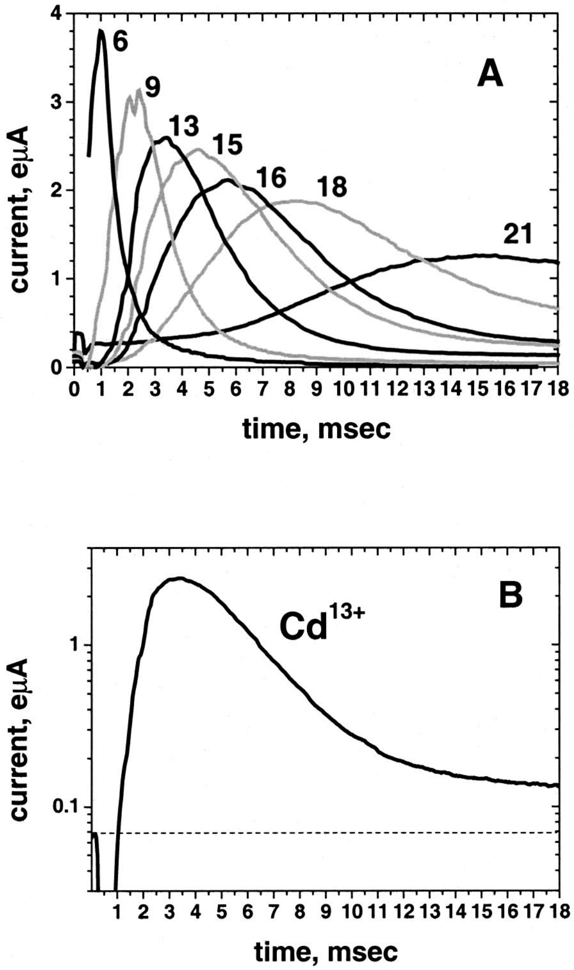

FIG. 2. (A) Pulses of cadmium ions generated after the injection of laser ablated fluxes into an argon ECRIS plasma. The charge states of the ions are indicated at their corresponding graphs. The laser unit was triggered at time $t = 0.25$ ms. (B) A pulse of Cd^{13+} ions presented in logarithmic scale to show more clearly its saturation at a level above the dc currents (indicated by dashed line).

obtained in these cases due to the limited time available for these tests. We plan to repeat these particular investigations.

III. EXPERIMENTAL RESULTS

Two main phenomena were observed when laser produced fluxes were injected into the ECR discharge: (a) pulsed currents of ions of the injected metals were generated; and (b) the ionic currents from the working gas deviated from their dc levels. The shapes of the pulses were clearly different for different charge states of metal ions, with shorter rise and fall times for lower charge states compared to those for highly charged ions. This behavior is illustrated in Fig. 2(A) for the production of Cd^{Z+} ions in an Ar plasma at the gas pressure of 1.5×10^{-7} mbar and 300 W of injected microwave power. The pressure was measured at the injection side of the source relatively close to the vacuum pump. The range of representation has been chosen such that the laser unit is triggered at 0.25 ms. Hence, the levels of the dc currents of Cd ions can be seen at the graph prior to this moment. It is interesting to note that at least two time constants are needed to describe the decay of the current pulses. To show this behavior more clearly, in Fig. 2(B) the pulse of Cd^{13+} ions is presented in logarithmic scale.

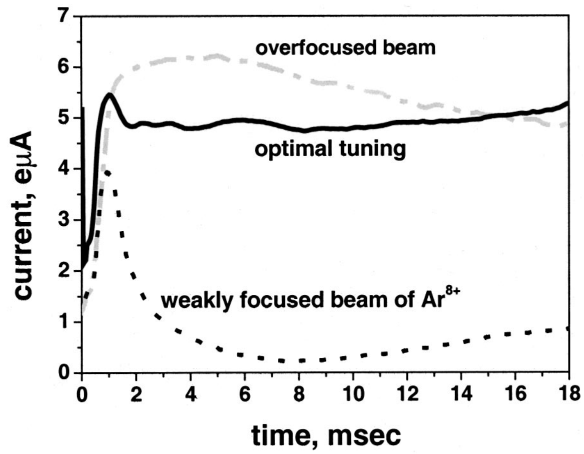

FIG. 3. Distortions of Ar^{8+} ion currents by the injection of laser ablated fluxes of magnesium atoms. The oscillograms are obtained with three different tunings of the beam transport line.

For high laser beam energies, i.e., for high fluxes of ablated material into the plasma, and for both types of ablated materials, distortions of the ion currents of the main gas (Ar^{Z+}) and of the dc component of Cd^{Z+} ions were observed. The time dependent shapes of these distortions were different for different tunings of the beam transport optics and for different charge states. This is demonstrated in Fig. 3. They also depended on gas pressure and microwave power. However, some characteristic features common to all distortions could be observed. Immediately after triggering the laser, the currents decreased for the high ion charge states (i.e., $Z \geqslant 6$ for argon ions), whereas the currents of the low charge states increased. This stage lasts about 0.5 ms. It is followed by a short increase of the currents, and then the disturbed currents recover relatively slowly to their initial dc levels. This recovery stage lasts about 20 ms. It occurs either from above the initial level of current (dash-dotted line in Fig. 3) or from below (dotted line), depending on the voltages at the Einzel and quadruple lenses in the beam transport line. The parameters of the beam optics could also be chosen such that almost no deviations in the currents were observed after the first, fast stage (solid line in Fig. 3).

When the energy of the laser beam was reduced to a level close to the ablation threshold, the influence of the laser ablated fluxes to the extracted ion currents became negligibly small, deviating now by less than 10% from their dc values after triggering the laser.

In contrast to this behavior of the dc ion currents, the time structure of the pulsed Cd(Mg) currents does not depend on the laser beam energy and, consequently, on the number of neutrals injected into the discharge (Fig. 4). Only the amplitudes of the currents change for different laser beam energies. Varying the parameters of the beam transport optics, small changes in the shape of the ionic pulses are observed, with $\pm 10\%$ variation in the rise time of the extracted currents. We assume that the disturbances of the extracted dc currents are not due to changes in the electron

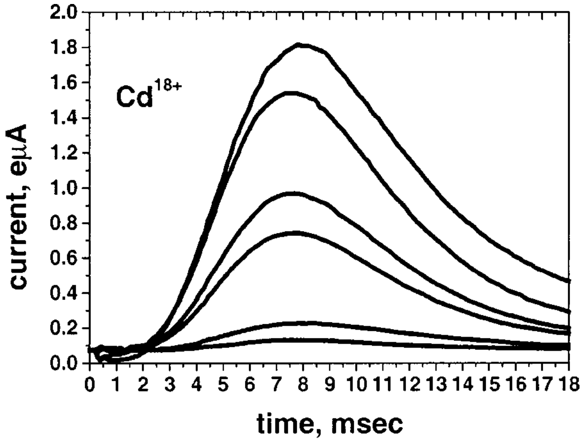

FIG. 4. Pulses of Cd^{18+} ions as obtained for different laser beam energies under fixed conditions of the ECRIS. The laser beam energies were varied in five steps from 5 (lower curve) to 30 mJ (upper curve).

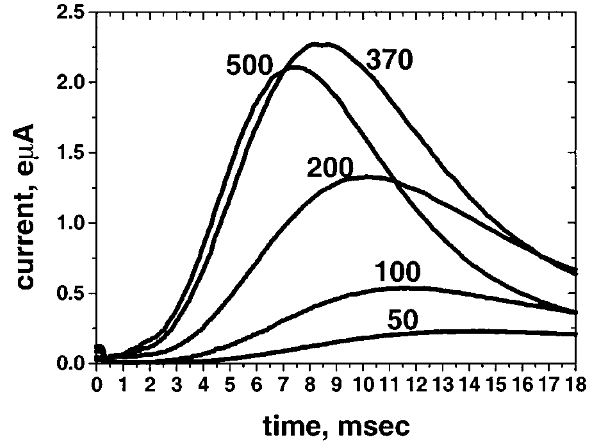

FIG. 5. Pulses of Cd^{18+} ions after injection of cadmium atoms into an argon ECR plasma for different microwave powers. The values of the microwave power are indicated at the graphs in units of watts. The argon pressure was 2.7×10^{-7} mbar.

density and temperature inside the dense core plasma, but rather have to be ascribed to changes in the transport/extraction conditions of the ions. In the following, we present pulsed currents of Cd(Mg) ions obtained at the maximum available laser beam energies.

In order to avoid plasma oscillations and instabilities due to extensive heating, we established the maximum microwave power to less than 500 W. In these conditions, the optimal pressure of Ar for the production of Ar^{8+}–Ar^{12+} ions in the Frankfurt ECRIS is in range of $(1.5–3)\times10^{-7}$ mbar. Simultaneously to the experiments on laser ablation, the dc output currents of Ar^{Z+} ions were also measured as a function of the microwave power. The measured currents of Ar^{Z+} are given in Table I. Also, in this table the currents of H_2^{1+} and Cd^{18+} are given representing those ion species, the fluxes of which are generated by sputtering off the chamber walls and the plasma electrode. For these experiments, no cadmium target was located inside the chamber for the measurements of dc currents. Cadmium atoms entered the discharge only via the contamination of the plasma chamber. The gas pressure in the source was about 2.7×10^{-7} mbar. The beam line optical elements were tuned for the transport of Ar^{8+}.

It is seen that 400 W of injected microwave power is an optimal value for the production of HCI under the present conditions of the source: an increase of the injected microwave power up to 400 W results in an increase of extracted Ar ions with $Z\geqslant7$ and in a decrease of the lower charge states. A further increase of the power to values larger than 400 W leads to a clear decrease in the extracted currents of the high charge states. Simultaneously, the currents of H_2^{1+} and Cd^{18+} ions, i.e., of the sputtered particles, increase under these conditions.

The rise/fall times of the pulsed currents of metal ions created by laser ablation get faster if the microwave power is increased. This is especially pronounced for ions with high charge states ($Z\geqslant10$, measurable under Cd injection). Figure 5 illustrates the typical dynamics of the slopes of the current pulses for the case of Cd injection into an argon plasma.

Also, for the pulsed currents an increase of the amplitudes of the pulses is observed when the microwave power is brought up from 50 to 400 W, whereas for higher microwave powers the amplitudes decrease again and become less stable. In Table II, the dependencies of the rise time of the pulsed currents of Mg^{5+} ions representing low charge states and Cd^{18+} representing high charge states as a function of the microwave power are presented. The source conditions were slightly different for both cases due to replacement of the target, which demanded an opening of the source between the two runs.

In these experiments, only very moderate changes were detected in the rise times of the ionic pulses for low charges (Mg^{5+}) when rising the microwave power above 50 W. The rise time of Mg^{5+} decreased from $\tau_{rise}=0.85$ to 0.75 ms (i.e., approximately by a factor of 1.1, Table II), when the microwave power is increased from 100 to 400 W. For Mg^{4+} ions, τ_{rise} was 0.4 ms in this range of microwave power. For the

TABLE I. Currents of Ar^{Z+}, H_2^{1+}, and Cd^{18+} ions measured in dc mode (without laser ablation inside the chamber) as a function of injected microwave power for constant argon pressure.

Power (W)	Electric current of ions (eμA)												
	Ar^{2+}	Ar^{3+}	Ar^{4+}	Ar^{5+}	Ar^{6+}	Ar^{7+}	Ar^{8+}	Ar^{9+}	Ar^{10+}	Ar^{11+}	Ar^{12+}	H_2^{1+}	Cd^{18+}
100	0.32	1.9	6.3	11.2	14.4	13.1	11.9	2.8	0.4	0.04	0.01	0.08	0.03
200	0.34	1.7	5.1	11.3	17.0	20.4	26.7	9.6	2.1	0.3	0.04	0.14	0.05
300	0.26	1.4	3.7	9.5	16.7	23.0	36.2	16.3	4.7	0.9	0.10	0.19	0.07
400	0.19	1.2	3.1	8.3	15.5	23.1	39.4	19.8	6.4	1.3	0.16	0.21	0.06
500	0.21	1.4	3.7	8.8	15.6	22.5	37.6	16.9	5.2	0.9	0.09	0.30	0.15

TABLE II. Total particle and electric currents of Ar^{Z+} ions, mean charge state of Ar^{Z+} ions in extracted currents, rise times for pulses of Mg^{5+} and Cd^{18+} ions as a function of injected microwave power for constant argon pressure.

Power (W)	Total particle current (I_p) (pμA)	Total electric current (I_e) (eμA)	$Z_{mean}=I_e/I_p$	Rise time of Mg^{5+} ion pulses (ms)	Rise time of Cd^{18+} ion pulses (ms)
100	10.7	62.5	5.8	0.85	12.0
200	14.7	94.8	6.5	0.80	10.0
300	16.4	112.9	6.9	0.75	9.0
400	16.7	118.6	7.1	0.74	7.8
500	16.2	113.3	7.0	0.73	7.5

higher charge states, the difference in the production rates was more pronounced: for Cd^{18+} ion pulses τ_{rise} decreased from 12 to 8 ms (i.e., by factor of ≅1.5) in the same range of power variation.

In the present status of tuning of the ECRIS, the mean charge state of Ar ions (Z_{mean}) gradually shifts to higher values with increasing microwave power (Table II), until the plasma becomes unstable above 400 W of injected microwave power. This instability manifests itself in a decrease of Z_{mean} and in a prominent increase in the extracted dc currents of H_2^{1+} and Cd^{18+} ions. Fluxes of neutral H_2 and Cd particles into the plasma are determined mainly by the desorption of molecules and atoms from the chamber walls and the plasma electrodes under ion impact. Thus, the extracted currents of these ions could be considered an indicator of how many HCIs hit the walls. These losses are clearly increased for rf powers of about or more than 400 W. It can be readily seen from Fig. 5 that the amplitude of Cd^{18+} pulses is decreased already noticeably at 500 W compared to 370 W.

Analyzing the charge state spectra of Ar^{Z+}, we calculate that the mean charge states are $Z_{mean}=7.0$ for 500 W, $Z_{mean}=7.1$ for 400 W, and $Z_M=5.8$ for 100 W of injected microwave power (Table II). The current of Ar^{8+} ions increases approximately by a factor of 3 when going from 100 to 400 W (Table I), and almost the same increase is observed for the amplitudes of Cd^{18+} pulses.

Figure 6 illustrates the variation of the rise times for Cd^{18+} ions (left scale) and Mg^{5+} ions (right scale) as a function of the source pressure. The microwave power was 300 W. The variations in τ_{rise} for Cd^{18+} are small at pressures larger than 1.5×10^{-7} mbar and become very large for low pressures. Also, for Mg^{5+} current pulses created in an argon discharge, the same tendency of τ_{rise} was observed, but the shape of the Mg^{5+} pulses is more strongly affected by changes of the gas pressure at values above 1.5×10^{-7} mbar. No saturation was observed for the rise times. The time structure of Cd^{18+} ion pulses (Fig. 7) reveals an increased level of fast oscillations in the extracted current for pressures above 2.3×10^{-7} mbar. Also, currents of other charge states of Cd and Ar ions oscillate above this pressure with amplitudes in a range of 10%–30%. Varying the gas pressure, dc currents of Ar^{12+} ions start to decrease already for pressures above 1.5×10^{-7} mbar, whereas Ar^{8+} currents increase up to pressures of 2.3×10^{-7} mbar and then decrease. Pulsed amplitudes of Cd^{18+} currents reach their maximum at pressure of 1.5×10^{-7} mbar at the same pressure as Ar^{12+} ion currents.

The ''gas-mixing'' mode of operation[12] has also been tested during the injection of Cd and Mg atoms into the ECR discharge. Controlled addition of oxygen into the source resulted in an increase of the output currents for Ar^{12+} and Ar^{11+} by factors of roughly 2, with a simultaneous decrease of the extracted currents of lowly charged argon ions ($Z \leqslant 8$). The pulse amplitudes of Cd/Mg ion currents decreased for all charge states, with a somewhat more pronounced de-

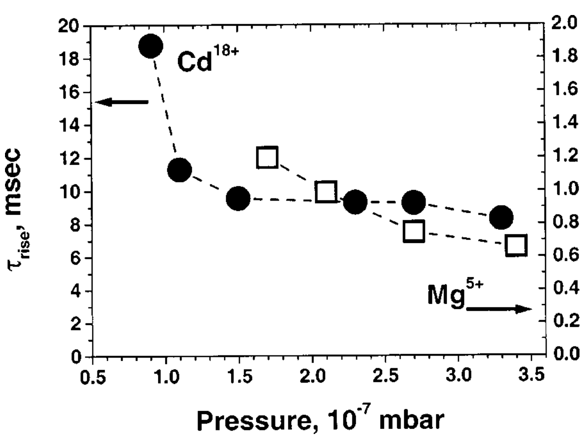

FIG. 6. Rise times of the current pulses of Cd^{18+} ions (closed circles, left scale) and Mg^{5+} (open squares, right scale) as a function of argon gas pressure, at a constant microwave power of 300 W.

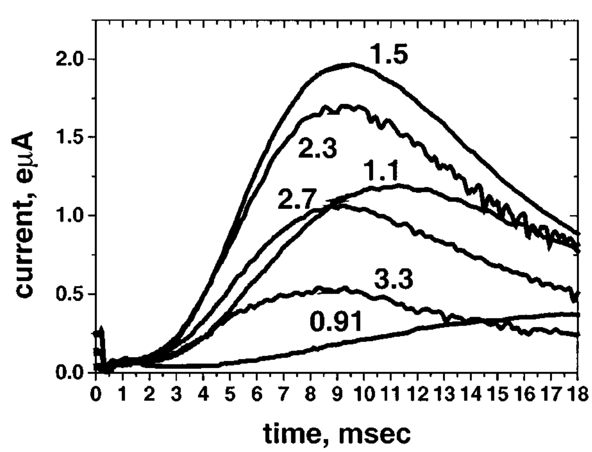

FIG. 7. Pulses of Cd^{18+} ions in a pure Ar discharge as a function of the gas pressure. The values of pressure are indicated at the graphs in units of 10^{-7} mbar. The microwave power is 300 W.

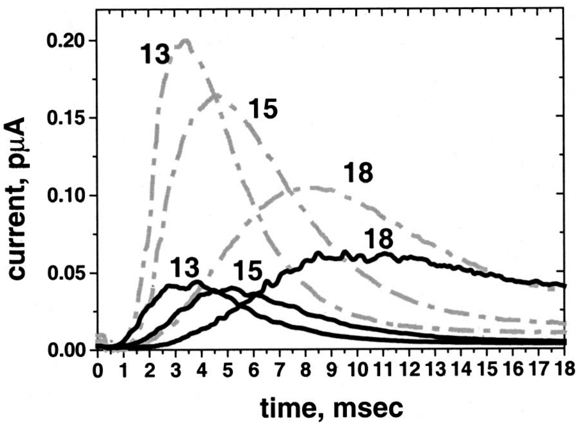

FIG. 8. Currents of $Cd^{13+,15+,18+}$ in pure argon plasma (dashed-dotted lines) and in oxygen gas-mixing mode (solid lines). The charge states of the ions are indicated at the graphs.

crease for the lower charge states. The rise times did not change noticeably. The pulses of Cd ions with $Z=13$, 15, and 18+ are presented in Fig. 8 for pure Ar as working gas optimized for the production of Ar^{12+} ions (pressure-1.5 $\times 10^{-7}$ mbar, microwave power–400 W, dash-dot lines at the graph), and for the operation in gas-mixing mode for the same power at a total gas pressure of 3.5×10^{-7} mbar. The gas mixture was optimized for the extraction of Ar^{12+} ions. Note that the currents are presented here in particle microamperes (pμA) to show the dynamics of particle losses more clearly.

The influence of the biased-electrode voltage on the shape of the ionic current pulses has also been investigated. As it has been reported already,[9] no changes were observed in the rise/fall times of the pulses. We also studied the influence of pulsing the biased-disk voltage[13] on the dynamics of metal ion production. In this case, without laser ablation, but exposing the Cd target to sputtering by the ECR plasma, a pulsed increase of Cd ion currents over their dc level was observed. This behavior was especially pronounced for the highest charge states. Pulses of Cd^{21+} ions with amplitudes exceeding the dc level by factors of 2–3, could be produced by switching the bias voltage from +300 to −500 V in a step-like manner for approximately equal periods of time with a bias modulation frequency of 1 kHz. A more detailed description of these measurements will be given in a forthcoming article.

IV. DISCUSSION

When the laser-ablated neutrals pass through the ECR plasma, they are ionized by electron impact. Being captured in the plasma, these lowly charged ions begin to increase their charge step by step in electron–ion collisions, whereas the total content of injected particles in the plasma gradually decreases due to ion losses to the walls and to ion extraction. The ionization times for ions are inversely proportional to $n_e\times\langle\sigma_Z v\rangle$, where n_e is effective density of electrons, and $\langle\sigma_Z v\rangle$ is the rate coefficient, i.e., the product of ionization cross section for an ion of charge state $Z+$ and electron velocity averaged over the distribution of the electron velocities. A higher electron density results in a shorter ionization time. The ionization cross-sections σ_Z decrease rapidly with increasing Z, and, in general, the higher the charge state of an ion, the longer will be the time that is required to produce it. The curves of Fig. 2 illustrate this step-by-step production of ions in the plasma, where different rise times for different charge states can be directly observed.

We carried out numerical calculations to simulate the ionization dynamics for magnesium ions using the fit formula for the rate coefficients $\langle\sigma_Z v\rangle$ given in Ref. 14, where Maxwellian velocity distributions are assumed. Unfortunately, the data of Ref. 14 are given only for elements up to Ni. Hence, we were not able to estimate the cadmium ion production in this simple model. Besides the loss channel of ionization, no other ion losses are taken into account in these calculations. The rise times for the creation of ion species at a given electron density inside the ECR plasma, as obtained by this simple approach, are presented in Table III for Mg ions of different charge states as a function of the mean electron temperature. The electron density was fixed to $n_e=7.5\times 10^{11}\ \mathrm{cm}^{-3}$. All calculations were started with the same level of density of neutral Mg atoms. No further dynamics of atom and electron densities, e.g., additional time dependent fluxes of neutrals into the plasma, had been taken into account. The extracted currents are directly proportional to the ion densities inside the plasma. The experimentally measured shapes of $Mg^{4+,5+}$ ion pulses as representatives of low charge state ions are best reproduced by assuming the above-mentioned electron density and an electron temperature in the range of 1–3 keV. No better fit of T_e is possible when only low charge states are analyzed.

From Table III, it can be deduced that the production

TABLE III. Model calculations of rise times for the ion densities of magnesium ions as a function of electron temperature. The electron density is $0.75\times 10^{12}\ \mathrm{cm}^{-3}$.

Electron temperature (T_e) (eV)	Calculated rise time of ion pulses (ms) Electron density—$0.75\times 10^{12}\ \mathrm{cm}^{-3}$				
	Mg^{4+}	Mg^{5+}	Mg^{6+}	Mg^{7+}	Mg^{8+}
200	0.83	1.94	4.64	8.61	⋯
400	0.52	1.13	2.33	4.03	8.46
500	0.48	1.01	2.03	3.4	7.21
750	0.42	0.87	1.69	2.79	5.53
1000	0.4	0.79	1.54	2.54	4.94
1500	0.4	0.75	1.42	2.32	4.5
2500	0.4	0.75	1.41	2.25	3.54

rates for low charge states of Mg ions (4+, 5+) are not affected by changes of the electron temperature at values above 400–500 eV. The higher the ion charge, however, the more pronounced is the influence of T_e on the ionization dynamics, and, e.g., for Mg^{8+} ions, the τ_{rise} values are not expected to saturate even at a T_e as high as 2500 eV. The ionization times are inversely proportional to the electron densities. Thus, at electron temperatures above 500 eV, the changes in the rise times of Mg^{5+} pulses, as shown, e.g., in Fig. 6, are indicative of changes in the electron density, rather than in the electron temperature.

Theoretical predictions of charge state spectra after injecting short pulses of Cd and Zn atoms into an argon ECR plasma have been obtained previously by solving the nonlinear set of balance equations for ion production/losses. The applied model is described in Ref. 15. It was found that the rise/fall times for the lowest charge states may be fitted by assuming mean electron temperatures $T_e = 0.5–1$ keV and electron densities of $n_e \approx 5 \times 10^{11}\ \mathrm{cm}^{-3}$ for the Frankfurt ECRIS.

Simulations of the bismuth–ion pulse dynamics for the Argonne PIIECR under laser ablation[2] resulted in an electron density in the range of $4 \times 10^{11} – 6 \times 10^{11}\ \mathrm{cm}^{-3}$ and electron temperatures between 1.5 and 4 keV. The rise time for Bi^{18+} was measured to be about 10 ms, quite close to our values for Cd^{18+} of 8 ms. It was also noted that the decay times of highly charged ions (Bi^{20+} and Bi^{24+}) could not be reproduced by simple electron-impact ionization/charge-exchange recombination models, but that ion escape processes also had to be taken into consideration. Indeed, for high charge states, the production/recombination processes are predicted to be in equilibrium. Hence, the decay of a pulse is determined by the escape of the ions from the plasma. The same observations were made when modeling the Cd ion dynamics in our previous publication.[6]

In contrast to the above, the dynamics of ions of low charge states is not determined by the ionic escape from the plasma, but by the ionization probabilities. However, as can be deduced from Fig. 2, at the latest stages of the ionization avalanche, when the density of the injected neutral particles should already be negligible, the currents of the cadmium ions with charge states above 9+ do not vanish completely. An almost constant slowly decaying level of extracted currents is observed. This indicates the important influence of charge-exchange and recombination processes on the production and quenching of the highest charge states of Cd ions. Apart from direct ionization, lowly charged ions are also produced from highly charged ones via these processes, which become dominant at a late stage of the pulse generation.

The effective electron density of $7.5 \times 10^{11}\ \mathrm{cm}^{-3}$, derived from our measurements, seems to be quite reasonable.[1] Almost the same value was measured recently in the Quadrumafios source[16] by means of microwave interferometry. There, the electron density n_e saturated as a function of microwave power at levels of $(3 \div 4) \times 10^{11}\ \mathrm{cm}^{-3}$ for microwave powers larger than 150 W and for relatively low gas pressures. For higher gas pressures, n_e increased with injected microwave power until values of approximately 600 W. For even higher powers, n_e decreased again.

In our experiments, we observed that the rise times of Cd/Mg current pulses always decreased with increasing gas pressure or injected microwave power. Lower ion charge states (Mg^{5+}) turned out to be more sensitive to changes of the gas pressure and exhibited only a rather weak dependence on the microwave power. In contrast to this, the pulse shapes for ions in higher charge states (Cd^{18+}) are affected most by changes in the microwave power level, not by changes in the gas pressure (Table II and Figs. 5 and 6). Setting a too high level of the microwave power or of the gas pressure resulted in a decrease of the output of HCI and in an excitation of plasma instabilities. However, no larger ionization times have been observed (Figs. 5 and 7).

From the above, we conclude that, for a fixed gas pressure, an increase of the microwave power does not result in a significant increase of the electron density but in an increase of the effective electron temperature enhancing the production of highly charged ions. When the gas pressure is increased, the electron density is increased too. From the fact that the rise time of Mg^{5+} ion pulses decreased by a factor of two when the gas pressure was increased from 1.7 to 3.4×10^{-7} mbar (Fig. 6), one can conclude that the ratio of the electron densities is roughly proportional to the ratio of gas pressures. The production rates of highly charged ions are not changed, however, which can be explained by a decrease of the electron temperature, which compensates the increase of the electron density. This is consistent with the results of simulation of ECR plasma given in Ref. 17.

The production rates for Cd ions are not changed significantly by adding oxygen into the argon ECR discharge. The decay times of the ion pulse for Cd^{18+} are noticeably increased, while the amplitudes of the pulses are strongly reduced, especially for cadmium ions with lower charge states. This indicates a reduction in the loss rates of ions during the ionization avalanche, and increased confinement of the ions in the plasma. More detailed studies of the dynamics are requested. However, for this purpose an improved stability of operation of the Frankfurt ECRIS is essential. We plan to continue these experiments.

ACKNOWLEDGMENTS

The Frankfurt 14 GHz ECRIS-(VE)-RFQ Facility is a HBFG project of the Hessisches Ministerium für Wissenschaft und Kultur (HMWK) and Deutsche Forschungsgemeinschaft (DFG) Project No. III P-23772-116-246. This work was performed in the frame of a collaboration supported by wissenschaftlich-technologische Zusammenarbeit (WTZ), Grant No. RUS-669-97, and Bundesministerium für Bildung und Forschung (BMBF), Grant No. BMBF 06OF-374. One of the authors (S.R.) is supported by Graduiertenkolleg ''Physik und Technik von Beschleunigern'' of the DFG.

[1] R. Geller, *Electron Cyclotron Resonance Ion Sources* (IOP, Bristol, 1996).
[2] R. C. Pardo, R. Harkewicz, and P. J. Billquist, Rev. Sci. Instrum. **67**, 1602 (1996).
[3] V. Mironov, G. Shirkov, O. Strekalovskiy, and N. Tokareva, Rev. Sci. Instrum. **69**, 1129 (1998).

[4] T. Okada, Y. Nakayama, W. K. A. Kumuduni, and M. Maeda, Appl. Phys. Lett. **61**, 2368 (1992).
[5] V. E. Mironov, S. M. Silnov, E. A. Sotnichenko, and B. A. Shestakov, JINR Communications, 9-83-536, Dubna, 1983 (in Russian).
[6] V. Mironov, O. Hohn, S. Runkel, L. Schmidt, G. Shirkov, K. E. Stiebing, H. Schmidt-Böcking, and A. Schempp, in Proceedings of the 14th International Workshop on ECR Ion Sources, ECRIS99, CERN, Geneva, 3–6 May 1999, CERN Report CERN/PS/99-52 (HP), 1999, p. 212.
[7] K. E. Stiebing, H. Streitz, L. Schmidt, A. Schremmer, K. Bethge, H. Schmidt-Böcking, A. Schempp, U. Bessler, P. Beller, and J. Madlung, Nucl. Instrum. Methods Phys. Res. B **113**, 34 (1996).
[8] L. Schächter, K. E. Stiebing, S. Dobrescu, Al. I. Badescu-Singureanu, S. Runkel, O. Hohn, L. Schmidt, A. Schempp, and H. Schmidt-Böcking, Rev. Sci. Instrum. **71**, 918 (2000).
[9] S. Runkel, O. Hohn, K. E. Stiebing, A. Schempp, H. Schmidt-Böcking, V. Mironov, and G. Shirkov, Rev. Sci. Instrum. **71**, 912 (2000).
[10] W. Yokota, Y. Saitoh, T. Nara, I. Ishii, K. Arakawa, and K. Ohkoshi, in Proceedings of the 14th International Workshop on ECR Ion Sources, ECRIS99, CERN, Geneva, 3–6 May 1999, CERN Report CERN/PS/99-52 (HP), 1999, p. 172.
[11] O. Hohn, S. Runkel, K. E. Stiebing, V. Mironov, G. Shirkov, S. Biri, L. Schächter, S. Dobresku, A. Schempp, and H. Schmidt-Böcking, in Proceedings of the 14th International Workshop on ECR Ion Sources, ECRIS99, CERN, Geneva, 3–6 May 1999, CERN Report CERN/PS/99-52 (HP), 1999, p. 180
[12] A. G. Drentje and J. Sijbring, KVI Annual Report, Groningen, 1983, p. 79; H. G. Mathews *et al.*, KFA Annual Report, Institut für Kernphysik, Jülich, 1983.
[13] S. Runkel, K. E. Stiebing, O. Hohn, V. Mironov, G. Shirkov, A. Schempp, and H. Schmidt-Böcking, in Proceedings of the 14th International Workshop on ECR Ion Sources, ECRIS99, CERN, Geneva, 3–6 May 1999, CERN Report CERN/PS/99-52 (HP), 1999, p. 183.
[14] G. S. Voronov, At. Data Nucl. Data Tables **65**, 1 (1997).
[15] G. Shirkov and G. Zschornack, *Electron Impact Ion Sources for Highly Charged Ions* (Vieweg and Sohn, Wiesbaden, 1996).
[16] C. Perret, A. Girard, H. Khodja, and G. Melin, Phys. Plasmas **6**, 3408 (1999).
[17] A. Girard, C. Pernot, G. Melin, and C. Lécot, Phys. Rev. E **62**, 1182 (2000).